



Hydration water molecules of nucleotide-free RNase T₁ studied by NMR spectroscopy in solution

Stefania Pfeiffer, Normann Spitzner, Frank Löhr & Heinz Rüterjans*

Institut für Biophysikalische Chemie, Johann Wolfgang Goethe-Universität, Biozentrum, N230, 1. OG, Marie-Curie-Straße 9, D-60439 Frankfurt, Germany

Received 30 June 1997; Accepted 29 August 1997

Key words: hydrogen bonds, protein hydration, ribonuclease T₁, water residence time

Abstract

The hydration of uncomplexed RNase T₁ was investigated by NMR spectroscopy at pH 5.5 and 313 K. Two-dimensional heteronuclear NOE and ROE difference experiments were employed to determine the spatial proximity and the residence times of water molecules at distinct sites of the protein. Backbone carbonyl oxygens involved in intermolecular hydrogen bonds to water molecules were identified based on $^1J_{\text{NC}'}$ coupling constants. These coupling constants were determined from 2D-H(CA)CO and ^{15}N -HSQC experiments with selective decoupling of the $^{13}\text{C}^\alpha$ nuclei during the t_1 evolution time. Our results support the existence of a chain of water molecules with increased residence times in the interior of the protein which is observed in several crystal structures with different inhibitor molecules and serves as a space filler between the α -helix and the central β -sheet. The analysis of $^1J_{\text{NC}'}$ coupling constants demonstrates that some of the water molecules seen in crystal structures are not involved in hydrogen bonds to backbone carbonyls as suggested by crystal structures. This is especially true for a water molecule, which is probably hydrogen bonded by the protonated carboxylate group of D76 and the hydroxyl group of T93 in solution, and for a water molecule, which was reported to connect four different amino acid residues in the core of the protein by intermolecular hydrogen bonds.

Introduction

Water molecules are essential for the stabilization of protein structure, for mediating polar interactions and for introducing flexibility to intermolecular interfaces (Jeffrey and Saenger, 1991; Wang et al., 1996). They connect different protein sites in the tertiary structure. When complexes are formed, water molecules must be removed from the binding sites which is often accompanied by an entropic effect. It is assumed that these water molecules support the gliding of ligands into the binding sites of a protein like a lubricant (Jeffrey and Saenger, 1991). Protein hydration was studied by various methods such as Raman, IR (infra-red) and NMR spectroscopy, calorimetry, X-ray and neutron diffraction and molecular dynamics simulations (Kuntz and Kautzmann, 1974; Finney, 1979; Finney et al., 1982,

1985; Edsall and McKenzie, 1983; Rupley et al., 1983; Piculle and Halle, 1986; Thanki et al., 1988; Westhof, 1993; Denisov and Halle, 1995a,b; Denisov et al., 1995).

Direct observation of protein hydration is possible by X-ray and neutron diffraction analysis. Protein molecules are not only hydrated in solution, but also in crystals, where 20% to 90% of the crystal volume may consist of water molecules (Jeffrey and Saenger, 1991). However, there are major differences between crystallographic studies and NMR investigations in solution. The detection of crystal water is independent on its residence time, but requires that a water molecule always returns to the same position (positionally ordered water molecules) thereby giving rise to an observable electron density (Levitt and Park, 1993). In general, hydration water molecules show excessive thermal motion. Water molecules seen in crystal structures are mostly directly or indirectly hydrogen-

*To whom correspondence should be addressed.

bonded, forming a network with other water molecules or polar backbone or side-chain groups of the protein. Usually, only the position of the water oxygen atom can be determined, whereas the orientations of the two O–H bonds mostly remain invisible (Jeffrey and Saenger, 1991). No information on kinetic parameters is available from crystal structures.

In contrast, the detection of water molecules by NMR spectroscopy does not require uniform ordering of the bound water molecules. Water molecules can be observed by through space magnetization transfer from water hydrogens to hydrogens of the protein (Otting and Wüthrich, 1989; Clore et al., 1990; Billeter, 1995). Therefore water molecules must reside at least several hundred picoseconds in close proximity ($\approx 4 \text{ \AA}$) of the protein. The exact position of the water molecule is not accessible. Dipolar interactions between spins leading to NOE (nuclear Overhauser effect) or ROE (rotating frame Overhauser effect) effects are not only dependent on the distance between corresponding spins but also on the correlation time of the interatomic vector in the static magnetic field B_0 . In case of intermolecular magnetization transfer the correlation time is approximately equal to the residence time (τ_{res}) of the water molecules near the protein. The ROE cross relaxation rate is positive for all correlation times, whereas the NOE cross relaxation rate changes sign at $\gamma_{\text{H}} B_0 \tau_{\text{res}} = 1.12$ (Solomon, 1955; Abragam, 1961; Bothner-By et al., 1985). Monitoring both ROE and NOE effects provides an estimate of the residence times of water molecules located near non-labile protons of the protein (Clore et al., 1990; Otting and Wüthrich, 1989; Otting et al., 1991). The accuracy of this measurement is limited as a consequence of several assumptions (Brüschweiler and Wright, 1994). Furthermore, an indirect magnetization transfer between water and the protein must be excluded using structural information and knowledge about the exchange rates of labile protons.

Water molecules are frequently attached to the protein by hydrogen bonds. There is a characteristic dependence of the $^1J_{\text{NC}}$ coupling constant of a peptide bond in solution on the nature of hydrogen bonds at either CO or NH groups of peptide groups (Klotz and Franzen, 1962; Berger, 1978; Walter and Wright, 1979; Eberhardt and Rains, 1994; Juranic et al., 1995). Hydrogen bond formation at the carbonyl oxygen increases the coupling constant about twice as much as hydrogen-bonding of amide protons decreases it. Molecular dynamics simulations of ubiquitin in water have shown that hydrogen-bonding to water has

a twofold larger impact on $^1J_{\text{NC}}$ than intraprotein hydrogen bonding (Juranic et al., 1996).

In this study, we investigated the hydration of nucleotide-free RNase T₁ (ribonuclease T₁) in solution employing multidimensional heteronuclear NMR spectroscopy. This enzyme has been a target of extensive biochemical and biophysical studies. RNase T₁ from the fungus *Aspergillus oryzae* consists of 104 amino acids (Takahashi, 1965) and cleaves single stranded RNA specifically at the 3' end of guanosine nucleotides (Egami et al., 1964; Egami, 1966; Egami and Nakamura, 1969). Guanosine monophosphates (for instance 2'GMP and 3'GMP) act as competitive inhibitors of this catalytic reaction. Base binding and catalysis occur in adjacent but different regions of the enzyme. The backbone amide protons of N43, N44 and Y45 as well as the carboxylate group of E46 and the backbone carbonyl of N98 are involved in the recognition of the guanine base (Heinemann and Saenger, 1982; Sugio et al., 1988). Thereby, the rings of Y42 and Y45 sandwich the guanine ring system. The amino acid residues H40, E58, R77 and H92 are located in close proximity to the phosphate group of the guanine nucleotide in protein-inhibitor-complexes. These amino acids are the catalytic centre of the enzyme (Takahashi et al., 1967; Takahashi, 1970, 1973, 1976; Arata et al., 1976; Nishikawa et al., 1987). The three-dimensional structure of nucleotide-free RNase T₁ is known from X-ray (Martinez-Oyanedel et al., 1991) as well as from NMR (Pfeiffer et al., 1997) and is characterized by an N-terminal two-stranded antiparallel β -sheet followed by an α -helix, and a central five-stranded antiparallel β -sheet (Figure 1). The cysteine residues 2 and 10 as well as 6 and 103 are connected by disulphide bridges.

Materials and methods

NMR spectra were recorded at 313 K with a Bruker DMX-600 spectrometer, equipped with a triple resonance probe tuned to ^1H , ^{13}C and ^{15}N resonance frequencies and a z -axis gradient facility. All experiments were performed with a uniformly $^{13}\text{C}/^{15}\text{N}$ labelled 2 mM RNase T₁ sample dissolved in 500 μl H_2O containing 8% D_2O at pH 5.5. The ^1H carrier was set on the water resonance frequency in all experiments.

NOE and ROE experiments

NOE and ROE experiments for the identification of water molecules near protein protons were performed

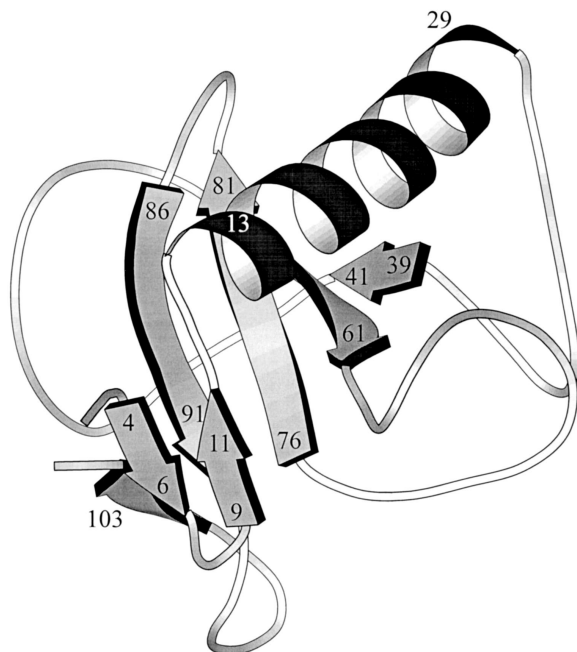


Figure 1. MOLSCRIPT drawing (Kraulis, 1991) of the tertiary structure of RNase T₁. For better orientation, some residues are indicated in the secondary structure elements by their sequence position. The N-terminal two-stranded antiparallel β -sheet comprises residues 4-6 and 9-11 followed by the α -helix including residues 13-29. The central five-stranded antiparallel β -sheet consists of the residues 38-40, 56-61, 76-81, 86-91 and 100-103.

separately for amide and aliphatic protons of the enzyme. The H₂O-ROE-¹⁵N-HSQC (heteronuclear single quantum coherence) experiment previously described by Grzesiek and Bax (1993b) was utilized for the observation of water molecules in the vicinity of the ¹⁵N bound protons of the protein. This experiment allows to distinguish between chemical exchange and magnetization transfer via ROE. The experiment comprises a selective inversion of the water resonance with a subsequent 90° pulse followed by a ROE mixing period. Two spectra are recorded in an interleaved mode, with the water magnetization aligned either parallel (+z) or antiparallel (-z) to the magnetization of all other ¹H spins before rotating it into the spin-lock axis. After the mixing period the magnetization is detected in an ¹⁵N-HSQC module. ¹⁵N-HSQC spectra were acquired with 512 real data points in the ¹⁵N dimension and 1024 complex data points in the acquisition domain with sweep widths of 3953.09 Hz (¹⁵N) and 8992.81 Hz (¹H), and a relaxation delay of 1.9 s. The ROE mixing time was 30 ms with an rf field strength of 4.5 kHz for the spin-lock pulse. Experiments used for detection of water molecules near aliphatic protons of

RNase T₁ followed the same principle. Pulse schemes of the H₂O-NOE-¹³C-ct-HSQC and H₂O-ROE-¹³C-ct-HSQC experiments were similar to those described by Grzesiek and Bax (1993a) and Clore et al. (1994) with addition of the WATERGATE flip-back method for water suppression (Piotto et al., 1992; Grzesiek and Bax, 1993a). The ¹³C-ct-HSQC spectra were acquired with 148 real data points in the ¹³C dimension and 768 complex data points in the acquisition domain with sweep widths of 10563.542 Hz (¹³C) and 8992.806 Hz (¹H), respectively. The relaxation delay was set to 1.8 s. The NOE and ROE mixing times were 60 ms and 30 ms, respectively. The spin-lock pulse for the ROE experiment had an rf field strength of 10 kHz.

¹J_{NC'} coupling constants

Two different types of 2D experiments were performed to determine the values of the ¹J_{NC'} coupling constants of RNase T₁. First, the ¹J_{NC'} coupling constants of the peptide bonds were observed using a ¹³C'-coupled ¹⁵N-HSQC experiment with a selective decoupling of the ¹³C^α carbons during the ¹⁵N evolution period as described previously (Delaglio et al., 1991) using the WATERGATE flip-back methodology for water suppression (Grzesiek and Bax, 1993a). Selective decoupling of the ¹³C^α carbons was achieved by an on-resonance G3-pulse with a duration of 256 μs. The spectrum was acquired with 900 real data points in the ¹⁵N dimension and 1024 complex data points in the acquisition domain using sweep widths of 2250.26 Hz (¹⁵N) and 8992.81 Hz (¹H). The relaxation delay was set to 1.0 s. Second, values of the ¹J_{NC'} coupling constant were extracted from gradient-selected 2D-H(CA)CO experiments with a selective decoupling of the ¹³C^α carbons during t₁ (Figure 2). Here, selective decoupling of the ¹³C^α carbons was obtained by an off-resonance G3-pulse with a duration of 1 ms. A total of eight 2D experiments were performed for the determination of the ¹J_{NC'} coupling constants:

- (1) 2D-¹⁵N-HSQC in H₂O at 313 K with selective ¹³C^α-decoupling during t₁,
- (2) 2D-H(CA)CO in H₂O at 313 K (pulse scheme in Figure 2),
- (3) 2D-H(CA)CO in D₂O at 313 K (pulse scheme in Figure 2),
- (4+5) 2D-H(CA)CO in H₂O at 313 K with ¹⁵N-decoupling during acquisition,
- (6+7) 2D-H(CA)CO in D₂O at 313 K with ¹⁵N-decoupling during acquisition,

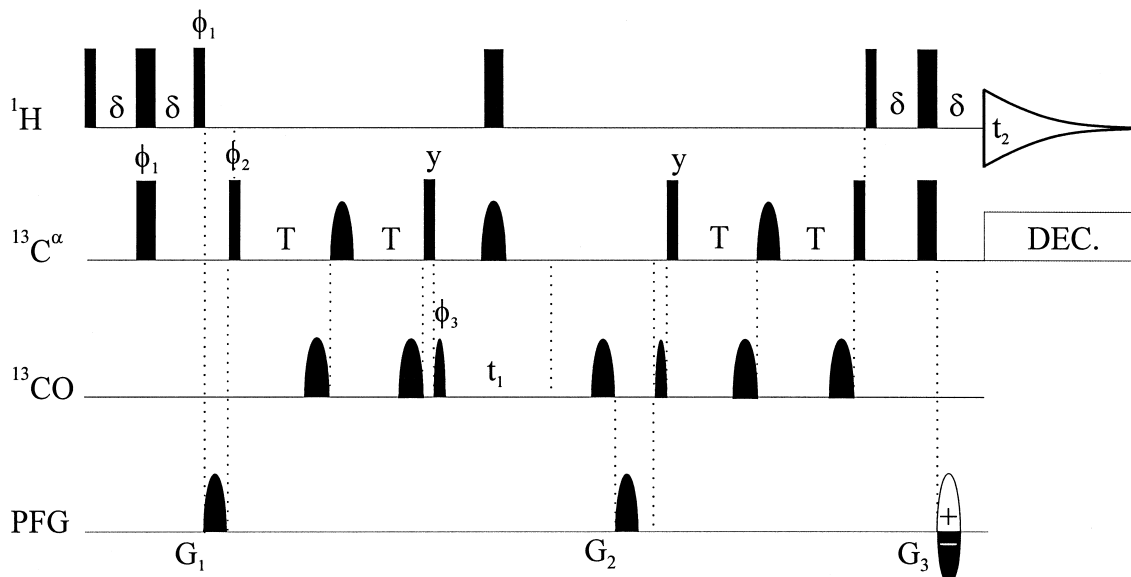


Figure 2. Pulse scheme of the 2D-H(CA)CO experiment for the measurement of the $^1J_{NC'}$ coupling constants. Narrow and wide pulses correspond to 90° and 180° flip angles, respectively. Pulses for which the phase is not indicated are applied along the x-axis. The ^1H carrier frequency is set to the H_2O resonance, the $^{13}\text{C}^\alpha$ and ^{13}CO carrier frequencies are set to 54 ppm and 174 ppm, respectively. The ^{13}C carrier is changed before and after the t_1 evolution period. ^{13}C decoupling is accomplished using GARP modulation with a 1.7 kHz rf field. Shaped pulses on ^{13}CO have the shape of the centre lobe of a $(\sin x)/x$ function and a duration of 124 μs . Shaped pulses on $^{13}\text{C}^\alpha$ nuclei are 1 ms G3-pulses. The first and last 180° pulse on $^{13}\text{C}^\alpha$ nuclei is applied with an rf power of 18.8 kHz. All other rectangular pulses on $^{13}\text{C}^\alpha$ nuclei are applied with reduced rf power of 4.6 kHz. The rf field strength is 26 kHz for all ^1H pulses. Pulsed field gradients have a sine-bell amplitude profile with a strength of $G_1 = 25$ G/cm, $G_2 = 44$ G/cm and $G_3 = 11.066$ G/cm at their centre. Their durations are $G_{1,2,3} = 2.5, 1.0, 1.0$ ms. Delay durations are $\delta = 1.7$ ms and $T = 4.0$ ms. Phase cycling is as follows: $\phi_1 = y, -y$; $\phi_2 = 2(x), 2(-x)$; $\phi_3 = 4(x), 4(-x)$; Acq. = $x, -x, -x, x, -x, x, x, -x$. Echo and anti-echo coherence transfer pathways are recorded alternatively by changing the sign of G_3 and combining the FIDs as described by Davis et al. (1992).

(8) 2D-H(CA)CO in D_2O at 308 K (pulse scheme in Figure 2).

Experiments 4 and 5 as well as 6 and 7 were identical. An experiment at 308 K was performed necessary to resolve overlapping correlation signals. All experiments were acquired with 800 real data points in the ^{13}C dimension and 384 complex data points in the acquisition domain with sweep widths of 2263.664 Hz (^{13}C) and 3592.954 Hz (^1H) using a relaxation delay of 1.0 s.

Data processing

The two interleaved data sets for the NOE and ROE experiments were separated using a simple C-program. The FIDs of the two corresponding data sets were multiplied in both dimensions by a cosine-bell function. After Fourier transformation, the data matrices of the experiment for the amide protons consisted of $1024(\omega_1) \times 2048(\omega_2)$ real data points, whereas the data matrices of the experiments for the aliphatic protons consisted of $1024(\omega_1) \times 1024(\omega_2)$

real data points. Subsequently, the two corresponding processed data sets were subtracted from each other.

The data matrices of all 2D experiments aimed to measure the $^1J_{NC'}$ coupling constants of the peptide bonds were multiplied with a cosine-bell window function in t_2 and with a 20° shifted sine-bell window function in t_1 prior to Fourier transformation. Finally, the spectra were zero-filled up to a size of 1024 real data points in ω_2 and 8096 real data points in ω_1 . The values of $^1J_{NC'}$ coupling constants were then obtained by the difference in the ^{15}N and ^{13}CO chemical shifts of the doublet components in ω_1 , respectively. In principle, all eight 2D experiments should give similar results. Therefore, the corresponding values of $^1J_{NC'}$ coupling constants were averaged over the experiments and averaged values were used for the further analysis.

Assignments of the resonance signals were based on the ^1H , ^{15}N and ^{13}C chemical shift values of RNase T₁ described previously (Pfeiffer et al., 1996). All spectra were evaluated using the programs XWIN-

NMR and AURELIA (Bruker Analytische Meßtechnik GmbH, Rheinstetten, Germany). Molecules were visualized using SYBYL (Tripos Inc., St. Louis, MO).

Results

ROE/NOE spectra of amide protons

The H₂O-ROE-¹⁵N-HSQC difference spectrum is shown in Figure 3. Three mechanisms were considered (Otting and Liepinsh, 1995) to give rise to cross peaks: (A) a direct ROE transfer between water and protein protons, (B) a ROE interaction between a protein proton and a rapidly exchanging proton, and (C) chemical exchange of the amide proton with water protons.

The ROE cross relaxation rate is always positive. This implies that the cross peaks in the difference spectrum are negative in case of mechanism A or B (Ernst et al., 1987). In contrast, a positive ROE cross peak implies that the magnetization transfer via chemical exchange dominates the interaction between the water protons and the amide protons of the protein, i.e. mechanism C (Table 1). Twenty-four backbone amide protons have positive cross peaks in the H₂O-ROE-¹⁵N-HSQC difference spectrum (Figure 3) and are assigned to class C. Class C cross peaks were also observed for the side-chain amide protons of N36, N43, R77, N83, Q85, N98 and N99. Measurements of the amide proton exchange rates at pH 5.5 and 313 K (Pfeiffer, 1997) have shown that nearly all of these amide protons have exchange rates greater than 1.0 s⁻¹ at pH 5.5.

Mechanisms (A) and (B) cannot be distinguished using relaxation data. The distinction was made by searching for rapidly exchanging protons in a 4.0 Å sphere around the considered protein protons in the solution structure of RNase T₁ (Pfeiffer et al., 1997). (This distance seems reasonable because one expects that the maximal distance observed by ROE interactions is not much larger than 3.5 Å based on signal-to-noise limitations.) The conformational space of RNase T₁ in solution was represented by 34 calculated conformers whereby the population of each conformer was not accessible. Therefore, each conformer was examined separately and only dipolar interactions for protein protons for which no rapidly exchanging proton fell in the 4.0 Å sphere in all conformers were considered as direct dipolar interactions with nearby water molecules. Rapidly exchanging protons were

supposed to comprise all hydroxyl protons of threonine, serine and tyrosine residues, and the labile protons of lysine, arginine and histidine residues. The only exception is the hydroxyl proton of Y11 which was observed in NOESY spectra with presaturation at 10.5 ppm, indicating that this hydroxyl proton is in slow exchange with water protons. Furthermore, the ¹H chemical shift difference of about 0.3 ppm compared to random coil (Liepinsh et al., 1992) suggests a hydrogen bond involving Y11 Hⁿ. In addition, all amide protons with class C cross peaks in the H₂O-ROE-¹⁵N-HSQC difference experiment (Figure 3) were considered to exchange sufficiently fast to cause a two-step magnetization transfer. Also all correlation signals in the difference spectrum which could potentially arise from an intramolecular dipolar interaction with the terminal NH₃ group or the amide proton of G70 at 4.84 ppm were omitted from the discussion. These amide protons might be selectively inverted together with the water proton resonance at 4.64 ppm. As indicated in Table 1, the backbone amide protons of S17, A19, E28, L62, V67, Y68, I90 and E102 and the side-chain amide protons of Q20 and W59 are at least 4.0 Å from all labile protons in the ensemble of the solution structure of RNase T₁ and were therefore classified as type A. These cross peaks identify unambiguously the spatial proximity of water molecules because the corresponding amide protons are well isolated from labile protons. The remaining cross peaks in Figure 3 were classified as type A/B since these amide protons are within 4.0 Å of rapidly exchanging protons of RNase T₁.

ROE/NOE spectra of aliphatic protons

The methyl region of the ¹³C-ct-HSQC reference spectrum of RNase T₁ is illustrated in Figure 4A, together with the corresponding region of the H₂O-NOE-¹³C-ct-HSQC and H₂O-ROE-¹³C-ct-HSQC difference spectrum (Figures 4B and 4C). Positive and negative correlation peaks in a ¹³C-ct-HSQC spectrum arise from an even and odd number of aliphatic carbon atoms next to the carbon nucleus of interest (Vuister and Bax, 1992). Since aliphatic protons are non-exchangeable, the sign of all ROE cross peaks in the difference spectrum (Figure 4A) is opposite to that observed in the reference spectrum. In case of a negative NOE cross relaxation rate the sign of the NOE cross peaks in the difference and in the reference ¹³C-ct-HSQC spectrum is identical (Figures 4A and 4B). Negative NOE cross relaxation rates between

Table 1. NOE and ROE cross peaks of type A and B (see text) and $^1J_{\text{NC}'}$ coupling constants listed along with the calculated distances of the closest labile proton in the solution structure and water oxygens being closest to the protein atom in the crystal structure of RNase T₁

Residue	Atom	$^1J_{\text{NC}'}$ ^a	Class ^b	Labile nearby ^c	Crystal water ^d
A1	O	16.6 ± 0 Hz	n.a.	n.a.	147 (3.68 Å)
	H ^β	n.a.	A/B	C2 H ^N (2.00 Å)	147 (2.78 Å)
C2	H ^{β2}	n.a.	A/B	T5 H ^{γ1} (1.97 Å)	136 (3.89 Å)
	H ^{β3}	n.a.	A/B	T5 H ^{γ1} (2.27 Å)	136 (2.89 Å)
D3	O	17.0 ± 0.5 Hz	n.a.	n.a.	136 (3.87 Å)
T5	HN	n.a.	A/B	T104 H ^{γ1} (2.00 Å)	136 (3.33 Å)
	H ^{γ2}	n.a.	A/B	T5 H ^{γ1} (2.00 Å)	175 (2.92 Å)
N9	H ^N	n.a.	A/B	S8 H ^N (2.39 Å)	167 (3.45 Å)
	H ^{β2}	n.a.	A/B	T5 H ^{γ1} (3.45 Å)	163 (4.20 Å)
	H ^{δ21}	n.a.	A/B	S8 H ^N (1.76 Å)	111 (3.03 Å)
	H ^{δ22}	n.a.	A/B	S8 H ^N (2.17 Å)	134 (2.97 Å)
C10	H ^{β2}	n.a.	A/B	T5 H ^{γ1} (2.37 Å)	163 (2.72 Å)
	H ^{β3}	n.a.	A/B	T5 H ^{γ1} (3.72 Å)	163 (3.60 Å)
S12	H ^N	n.a.	A/B	S12 H ^γ (2.00 Å)	122 (3.63 Å)
S13	H ^N	n.a.	A/B	S13 H ^γ (2.00 Å)	120 (3.29 Å)
D15	H ^N	n.a.	A/B	S12 H ^γ (2.00 Å)	123 (3.64 Å)
V16	H ^{γ1}	n.a.	A/B	Y4 H ⁿ (2.86 Å)	153 (3.14 Å)
	H ^{γ2}	n.a.	B	Y4 H ⁿ (2.76 Å)	>4.5 Å
S17	H ^N	n.a.	A		153 (3.30 Å)
T18	H ^N	n.a.	B	T18 H ^{γ1} (1.99 Å)	>4.5 Å
	H ^{γ2}	n.a.	A/B	T18 H ^{γ1} (2.44 Å)	158 (2.51 Å)
A19	H ^N	n.a.	A		110 (3.50 Å)
	H ^β	n.a.	A		110 (2.92 Å)
Q20	H ^{ε2}	n.a.	A		156 (3.01 Å)
K25	H ^ε	n.a.	A/B	K25 H ^ε (2.18 Å)	148 (4.41 Å)
E28	H ^N	n.a.	A		133 (5.66 Å)
D29	O	16.3 ± 0.4 Hz	n.a.	n.a.	202 (2.77 Å)
G30	O	16.6 ± 0.1 Hz	n.a.	n.a.	176 (3.86 Å)
T32	H ^N	n.a.	A/B	T32 H ^{γ1} (1.93 Å)	225 (3.26 Å)
	H ^{γ2}	n.a.	A/B	T32 H ^{γ1} (2.00 Å)	141, 116 (3.05 Å)
V33	H ^{γ1}	n.a.	A		222 (2.79 Å)
	H ^{γ2}	n.a.	A/B	G70 H ^N (1.98 Å)	191 (3.65 Å)
N36	H ^{β2}	n.a.	A/B	G71 H ^N (1.89 Å)	151 (3.57 Å)
K41	H ^ε	n.a.	A/B	N43 H ^{δ2} (1.93 Å)	126 (4.12 Å)
F50	H ^N	n.a.	A/B	49 H ^N (3.34 Å)	224 (2.53 Å)
S51	O	16.8 ± 0.2 Hz	n.a.	n.a.	>5.0 Å
V52	H ^{γ2}	n.a.	A/B	Y56 H ⁿ (3.03 Å)	196 (3.04 Å)
S54	H ^N	n.a.	B	S54 H ^γ (1.99 Å)	>4.5 Å
	H ^α	n.a.	B	S54 H ^γ (3.40 Å)	>4.5 Å
Y56	H ^N	n.a.	A/B	N43 H ^{δ2} (2.52 Å)	126 (1.93 Å)
W59	H ^{ε1}	n.a.	A		107 (2.44 Å)
I61	H ^N	n.a.	A/B	R77 H ⁿ (2.68 Å)	106 (3.93 Å)
	H ^{γ2}	n.a.	A		106 (4.72 Å)
L62	H ^N	n.a.	A		108 (2.02 Å)
	H ^{δ1}	n.a.	A		135 (2.94 Å)
	H ^{δ2}	n.a.	A/B	Y56 H ⁿ (2.00 Å)	106 (3.08 Å)

Table 1. Continued.

Residue	Atom	$^1J_{NC}$ ^a	Class ^b	Labile nearby ^c	Crystal water ^d
G65	H ^N	n.a.	A/B	S64 H ^N (2.01 Å)	113 (3.28 Å)
	O	16.4 ± 0.2 Hz	n.a.	n.a.	124 (2.91 Å) 203 (2.92 Å)
D66	H ^N	n.a.	B	S64 H ^N (3.36 Å)	>4.5 Å
V67	H ^N	n.a.	A		166 (1.95 Å)
	H ^{γ1}	n.a.	A/B	K25 H ^ε (3.00 Å)	191 (3.15 Å)
	H ^{γ2}	n.a.	A/B	K25 H ^ε (3.04 Å)	203 (3.19 Å)
Y68	H ^N	n.a.	A		107 (1.93 Å)
S69	H ^N	n.a.	A/B	S69 H ^γ (1.92 Å)	135 (1.89 Å)
G70	O	16.9 ± 0.3 Hz	n.a.	n.a.	182 (2.70 Å) 135 (2.76 Å)
	H ^{β2}	n.a.	A/B	G74 H ^N (1.91 Å)	115 (3.72 Å)
	H ^{β3}	n.a.	B	R77 H ^η (2.04 Å)	>4.5 Å
	H ^γ	n.a.	A/B	R77 H ^η (2.82 Å)	151 (2.88 Å)
A75	H ^β	n.a.	A/B	T91 H ^{γ1} (2.00 Å)	134 (2.63 Å)
D76	H ^N	n.a.	A/B	A75 H ^N (1.92 Å)	106 (2.00 Å)
R77	H ^{δ2}	n.a.	B	G74 H ^N (2.20 Å)	>4.5 Å
	H ^{δ3}	n.a.	A/B	R77 H ^η (1.90 Å)	121 (4.35 Å)
V79	H ^{γ1}	n.a.	B	N43 H ^N (3.40 Å)	>4.5 Å
N81	H ^{β2}	n.a.	B	N83 H ^{δ2} (1.93 Å)	>4.5 Å
N83	O	16.3 ± 0 Hz	n.a.	n.a.	173 (3.93 Å)
N83	H ^{β2}	n.a.	A/B	N83 H ^{δ2} (2.15 Å)	173 (2.91 Å)
	H ^{β3}	n.a.	A/B	N83 H ^{δ2} (3.39 Å)	201 (4.13 Å)
L86	H ^{δ2}	n.a.	A/B	Y4 H ^η (2.20 Å)	220 (3.14 Å)
V89	H ^{γ1}	n.a.	A		169 (5.50 Å)
I90	H ^N	n.a.	A		169 (5.80 Å)
	H ^{δ1}	n.a.	B	Y42 H ^η (2.16 Å)	>4.5 Å
T91	H ^{γ2}	n.a.	A/B	T91 H ^{γ1} (2.11 Å)	117 (3.19 Å)
T93	H ^N	n.a.	A/B	T91 H ^{γ1} (2.00 Å)	111 (4.38 Å)
	H ^{γ2}	n.a.	A/B	G94 H ^N (2.00 Å)	167 (2.76 Å)
G94	O	17.0 ± 0.2 Hz	n.a.	n.a.	146 (2.66 Å)
A95	H ^β	n.a.	A/B	N99 H ^{δ2} (2.00 Å)	215 (2.88 Å)
N98	O	16.5 ± 0.5 Hz	n.a.	n.a.	194 (3.17 Å)
E102	H ^N	n.a.	A		138 (1.87 Å)

^a The given coupling constants are mean values averaged over and standard deviations derived from eight experiments as described in Materials and methods.

^b Cross peak classification as described in Results. Dipolar interactions for protein protons which are close to labile protein protons but more than 4.5 Å away from a water oxygen were classified as type B.

^c The labile protons within 4.5 Å (in case of a NOE) and 4.0 Å (in case of a ROE) of the proton listed in the second column. Interproton distances were calculated in all 34 conformers of the solution structure of RNase T₁. Only the closest labile proton within the ensemble is listed.

^d Hydrogen atoms were built onto the heavy atoms of the protein using SYBYL software. Distances were calculated between the protein atoms listed in the second column and the water oxygens in the crystal structure. Because of the uncertainties in the orientation of the water protons and in the water oxygen atom coordinates, these distances have average uncertainties of 1.0–2.0 Å. Only the closest water oxygen is listed.

n.a. means ‘not applicable’.

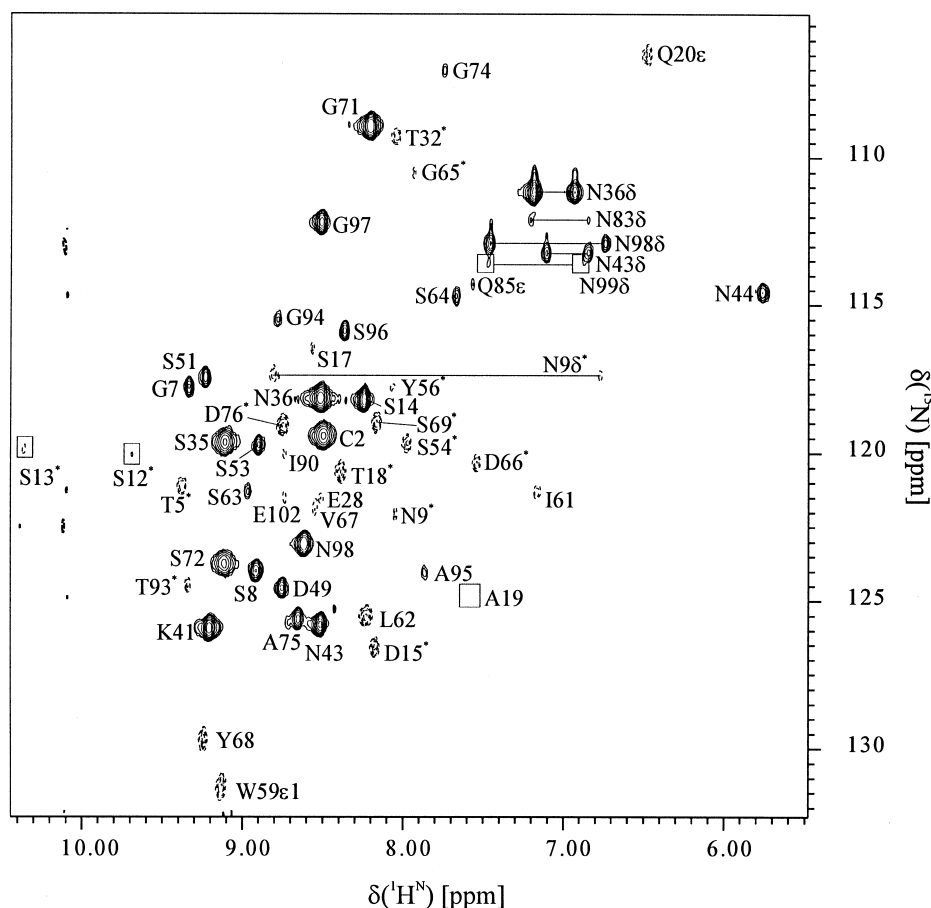


Figure 3. The H₂O-ROE-¹⁵N-HSQC difference spectrum of uniformly ¹⁵N/¹³C-labelled RNase T₁ recorded with a mixing time of 30 ms. Total acquisition time was 10 h. Dashed contours indicate negative intensities. Contours are spaced by a factor of 1.3. The amide correlation peaks are assigned with one-letter amino acid code and residue number. Negative cross peaks which arise not exclusively from direct water-protein contacts (see text) are marked with an asterisk. The correlation signals of G70 and R77 are outside of the displayed spectral region. The intensity of the correlation signals of A19 and the side-chain amide protons of N99 is smaller than the chosen threshold.

water molecules and the aliphatic (non-exchangeable) protons indicate residence times of water molecules of more than 300 ps (Otting and Wüthrich, 1989). Since the ROE cross relaxation rate is always positive, cross peaks appear in the H₂O-ROE-¹³C-ct-HSQC spectrum (Figure 4C) for dipolar interactions between the protein and water molecules with residence times of approximately 300 ps, whereas the NOE cross relaxation rate vanishes for this correlation time at a spectrometer frequency of 600 MHz ($\omega_0\tau_{\text{res}} \approx 1.12$). Cross peaks in the difference spectra within ± 1.5 ppm of the water resonance were omitted in the analysis because of baseline distortions due to the incomplete water suppression. Examination of Table 1 shows that 5 of the aliphatic cross peaks were caused by direct dipolar interactions with water molecules. They were

classified as type A. These aliphatic protons are also at least 4.5 Å from the closest labile proton in the solution structure of RNase T₁. The remaining cross peaks were classified as type A/B or B.

Intermolecular hydrogen bonds

Representative parts of the ¹³C'-coupled ¹⁵N-HSQC and the ¹⁵N-coupled 2D-H(CA)CO spectrum of RNase T₁ are shown in Figures 5A and 5B, respectively. Out of 103 values of ¹J_{NC'} coupling constants, 102 could be obtained. The missing value belongs to the peptide bond between the residues 69 and 70. The coupling constants range from 13.2 Hz to 17.0 Hz. Juranić et al. (1996) derived an equation for the dependence of the ¹J_{NC'} coupling constants from intermole-

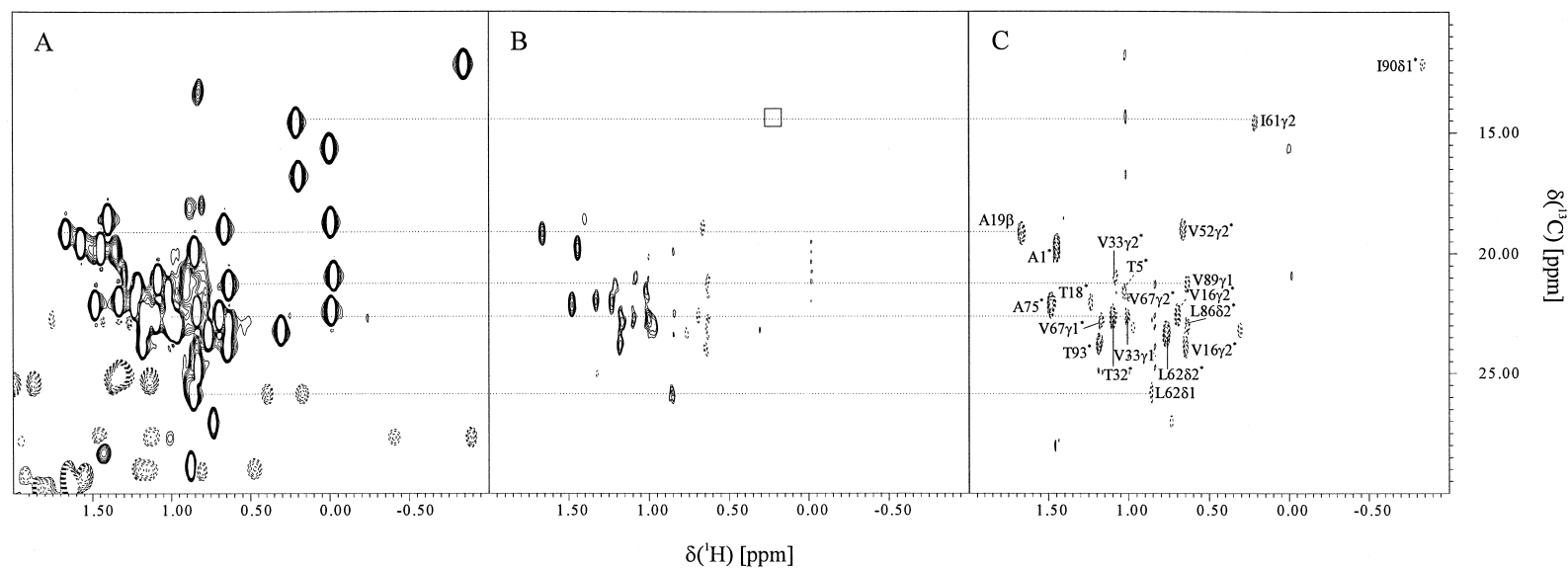


Figure 4. Methyl region of the ^{13}C -ct-HSQC reference spectrum (A), the H_2O -NOE- ^{13}C -ct-HSQC difference spectrum (B), and the H_2O -ROE- ^{13}C -ct-HSQC difference spectrum of RNase T₁ (C). The NOE and ROE experiments were recorded with mixing times of 60 ms and 30 ms, respectively, with total acquisition times of 12.5 h and 21.5 h. The correlation peaks are assigned with one-letter amino acid code and residue number. In case of isopropyl groups, the stereospecific assignment is given. Solid lines indicate positive peaks, dashed lines indicate negative peaks. Contours are spaced by a factor of 1.4. The reference spectrum (A) is plotted at a 10-fold higher contour level than the difference spectra (B) and (C). Peaks which arise not exclusively from direct water-protein contacts (see text) are marked with an asterisk. The correlation signals of direct water-protein interactions are connected by horizontal lines in the different experiments.

cular as well as from intramolecular hydrogen bonds $J(\text{hb})$:

$$J(\text{hb})/\text{Hz} = 14.3 + 4.1(\text{CO}_{\text{inter}}) + 1.6(\text{CO}_{\text{intra}}) \\ - 2.1(\text{NH}_{\text{inter}}) - 0.8(\text{NH}_{\text{intra}})$$

The correlation shows a dominant role of intermolecular $\text{C}=\text{O}\cdots\text{HOH}$ protein-solvent hydrogen bonds (CO_{inter}) on the $^1J_{\text{NC}'}$ coupling constant. High values of the $^1J_{\text{NC}'}$ coupling constant were described as unambiguous indicators for the high population of hydrogen bonds between water hydrogens and the protein backbone carbonyl oxygen (Juranić et al., 1995, 1996). We chose a cut-off value of $^1J_{\text{NC}'} > 16.2$ Hz for the average values of the $^1J_{\text{NC}'}$ coupling constants, because no $^1J_{\text{NC}'}$ coupling constant below 16.0 Hz was determined for the corresponding peptide bonds. The maximum standard deviation of these large $^1J_{\text{NC}'}$ coupling constants was 0.5 Hz. From this analysis it was concluded that the backbone carbonyl oxygen of residues 1, 3, 29, 30, 51, 65, 70, 83, 94 and 98 unambiguously accept intermolecular hydrogen bonds from water molecules. For all of these acceptors no or only slightly populated intramolecular hydrogen bonds were detected in the solution structure of RNase T₁ (supplementary material in Pfeiffer et al., 1997). Generally, CO sites may accept two hydrogen bonds. Thus, one intramolecular hydrogen bond within the protein involving a backbone carbonyl oxygen not necessarily excludes a second hydrogen bond between the oxygen and a water proton.

Values of $^1J_{\text{NC}'} < 14$ Hz may indicate the absence of intermolecular hydrogen bonds at the carbonyl site of the peptide bond. For five peptide bonds average $^1J_{\text{NC}'}$ coupling constants smaller than 14 Hz were obtained: S12–S13 (13.5 ± 0.3 Hz), Y42–N43 (13.2 ± 0 Hz), E58–W59 (13.4 ± 0.2 Hz), L62–S63 (13.4 ± 0.4 Hz) and N81–E82 (13.5 ± 0.3 Hz). These decreased $^1J_{\text{NC}'}$ coupling constants might be hints to hydrogen bonds between the amide proton of the peptide bond and a water molecule provided that intraprotein hydrogen bonds involving the NH site of these peptide bonds do not exist.

Application of the NMR data to the crystal structure

In the crystal structure of nucleotide-free RNase T₁ (Martinez-Oyanedel et al., 1991) 121 positions of water oxygen atoms were reported. A number of 30 water molecules was considered to be conserved in crystal structures of RNase T₁ with different inhibitors (Malin et al., 1991). Taking also three-centered hydrogen

bonds into account (Martinez-Oyanedel et al., 1991) we considered in the crystal structure of nucleotide-free RNase T₁ all water oxygens which are less than 4.0 Å away from carbonyl oxygens of peptide bonds with a coupling constant $^1J_{\text{NC}'} > 16.2$ Hz. This distance includes 1.0 Å for the H–O bond whose orientation is unknown in the crystal. In case of dipolar interactions, we considered all water molecules which are less than 6.0 Å away from protein protons for which direct NOE or ROE interactions were observed. This distance accounts for the unknown orientation of the O–H bond and the uncertainty of the atomic coordinates of the water oxygen atoms of about 1.0 Å. Table 1 shows the water molecules closest to the corresponding protein atoms in the crystal structure. In this way, 22 out of the 121 crystal water molecules were unambiguously supported by the NMR data in solution. They are associated with temperature factors of 6.6–50.57 Å² in the crystal. We see three different reasons why the remaining water molecules in the crystal cannot be identified by NMR spectroscopy: (1) They are more than 4.5 Å away from aliphatic or amide protons of the protein. (2) They are less than 4.5 Å away from aliphatic or amide protons of the protein, but these protein protons themselves are less than 4.5 Å away from rapidly exchanging protein protons (Table 1). (3) The residence time of these water molecules is too short for the observation of intermolecular dipolar interactions (shorter than 50–100 ps).

Discussion

The following discussion will focus on distinct hydration sites of RNase T₁ observed by NMR which correspond to conserved water molecules in crystal structures or to water molecules to which special attention was paid in the crystal structure analysis of the nucleotide-free enzyme.

A hydrogen-bonded chain of 10 conserved water molecules was described in crystal structures of RNase T₁ with different inhibitor molecules (Malin et al., 1991). Four of these water molecules were also described in the crystal structure of the nucleotide-free RNase T₁ (Martinez-Oyanedel et al., 1991): water molecules 107 (122), 108 (123), 110 (120) and 113 (116). Numbers in brackets correspond to the numbering of water molecules in Malin et al. (1991). The chain of these four water molecules is anchored at W59 H^{ε1} and stabilizes the loop structure formed by residues 60–68 in the crystal structures (see Figure 1).

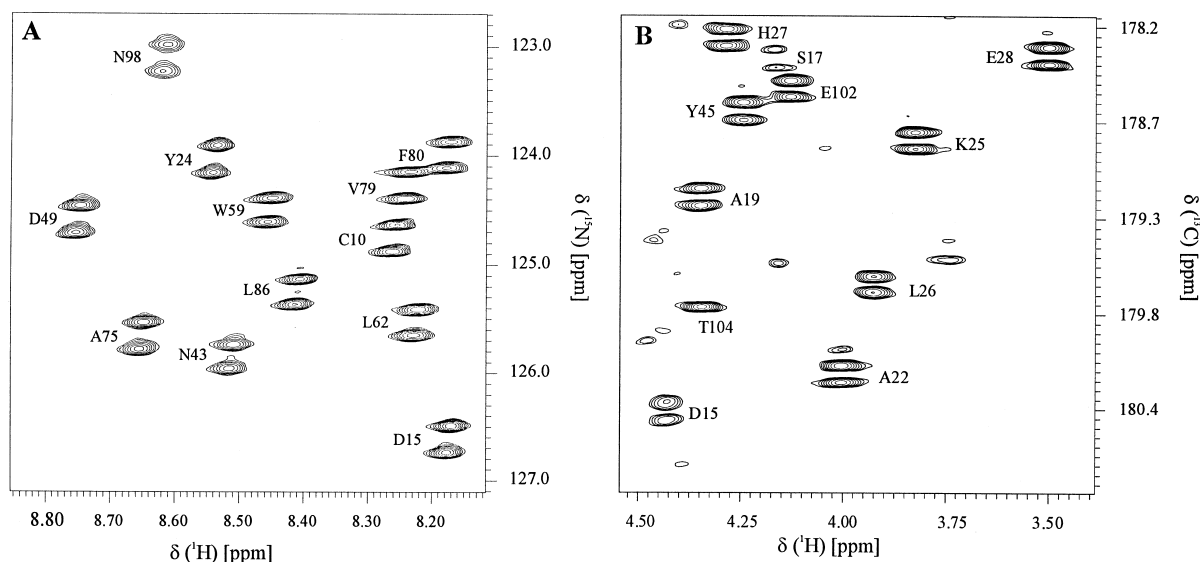


Figure 5. Region from the $^{13}\text{C}'$ -coupled ^{15}N -HSQC (A) and the ^{15}N -coupled 2D-H(CA)CO spectrum (B) of uniformly $^{15}\text{N}/^{13}\text{C}$ -labelled RNase T₁ recorded with $t_{1,\text{max}} = 200$ ms and 178 ms, respectively. The total acquisition time was 8 h for spectrum (A) and 4.3 h for spectrum (B). Data were processed using an exponential filter function in the t_1 domain and zero-filled to yield digital resolution of 0.2 Hz per data point in the ω_1 dimension. The $^1J_{\text{NC}'}$ coupling constants were obtained from the difference of the doublet components in ω_1 measured in Hz.

The mutation of W59 to Y doubles the catalytic activity of RNase T₁. All of these water molecules have low temperature factors. Water 107, 108 and 110 form hydrogen bonds with protein amide protons whereas the water molecule 113 was supposed to form a hydrogen bond with the backbone carbonyl group of L62 in the crystal. Indeed, dipolar interactions were observed for water 107/W59 $\text{H}^{\epsilon 1}$, water 108/L62 H^{N} , water 108/Y68 H^{N} , water 110/A19 H^{N} as well as for water 110/A19 H^{β} in solution. These three water molecules are buried and the corresponding cross peaks of A19 H^{β} , W59 $\text{H}^{\epsilon 1}$, L62 H^{N} and Y68 H^{N} are comparably strong as depicted in Figures 3 and 4. The solvent exchange rates of these three amide protons range between 10^{-4} s^{-1} and 10^{-6} s^{-1} (slow exchange). No or less populated intramolecular hydrogen bonds were detected for these amide protons in the solution structure of RNase T₁ (Pfeiffer et al., 1997). The NOE cross peak for A19 H^{β} is associated with a negative cross relaxation rate. In summary, this indicates short water-protein distances and residence times greater than 300 ps (Otting and Wüthrich, 1989). This observation is consistent with the crystal structures in which the mentioned ^{15}N -bound protons (except A19 H^{N}) are involved in intermolecular hydrogen bonds with the described conserved internal water molecules 107, 108 and 110. The proposed hydrogen bonds between the water molecules 107, 113 and 108

and the backbone carbonyl oxygens of P60, L62 and D66, respectively, cannot be confirmed by the NMR data: The values of the $^1J_{\text{NC}'}$ coupling constants of the corresponding peptide bonds are 15.4 ± 0.3 Hz, 13.4 ± 0.4 Hz and 15.0 ± 0.4 Hz, which would be in contradiction to a high population of intermolecular hydrogen bonds at these CO sites. Although water 113 is within 3.5 \AA of I61 $\text{H}^{\gamma 1}$ and $\text{H}^{\delta 1}$, no dipolar interactions were observed. These observations suggest that the residence time of water 113 is only a few hundred picoseconds.

In several crystal structures (Malin et al., 1991), two of the 10 water molecules interact with the N-terminal side-chains of the α -helix. In solution, a dipolar interaction was detected between the water molecule 153 and S17 H^{N} . Water 153 (117) was also described to be conserved. The ROE cross peak for S17 H^{N} is very weak implying a larger distance to the water 153 and a rather short residence time of a few hundred picoseconds.

Water 106 has the lowest temperature factor in the crystal structure of nucleotide-free RNase T₁. It donates two hydrogen bonds, to I61 O and P73 O, and accepts two hydrogen bonds, from A75 H^{N} and D76 H^{N} (see Figure 1). A ROE but no NOE cross peak was observed between this water molecule and I61 $\text{H}^{\gamma 2}$. The absence of a NOE cross peak suggests a residence time of about 300 ps. All other potential contacts be-

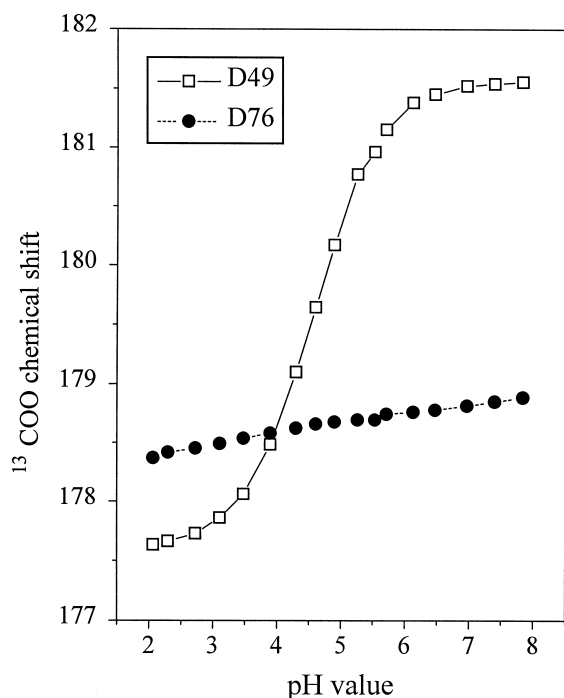


Figure 6. Titration curve of the carboxylate group of D76 monitored by NMR spectroscopy using a 2D H(CA)CO experiment (Kay et al., 1990) which correlates the ^1H chemical shifts of the preceding β -methylene protons with the ^{13}C chemical shifts of the carboxylate carbon nucleus (^{13}COO). The variation of the ^{13}C chemical shift dependent on the pH value is shown for D76 in comparison with D49. A ^{13}C chemical shift value of 175–178 ppm is expected for protonated carboxylate groups, whereas a value of 180–182 ppm is expected for deprotonated carboxylate groups of RNase T₁. Further details of the titration will be described elsewhere (N. Spitzner, to be published).

tween the protein and water 106 are ambiguous owing to the proximity of labile protons like the amide proton of A75, which shows a strong positive ROE cross peak. The proximity of A75 H^{N} led to a classification of the very strong and negative ROE cross peak for D76 H^{N} as type A/B. The $^1J_{\text{NC}}$ coupling constants for the peptide bonds involving I61 O and P73 O exhibit no extreme values. At best, the value for P73 is slightly increased (16.0 ± 0.3 Hz). Thus, some or all of the proposed intermolecular hydrogen bonds to backbone carbonyls are absent in solution.

Attention was paid to the conserved water molecule 111 (111) in the structure for RNase T₁. It was reported to be completely buried in crystal structures and could be hydrogen bonded to D76 $\text{O}^{\delta 1}$, to T93 $\text{H}^{\gamma 1}$ and T93 $\text{O}^{\gamma 1}$ (see Figure 1). In the crystal structure (Martinez-Oyanedel et al., 1991) the backbone carbonyl oxygen of C6 might also serve as hydrogen bond

acceptor regarding the distance of 3.05 Å between the two oxygen atoms. The observable protein protons within 3.5 Å of water 111 comprise C6 $\text{H}^{\beta 2}$, N9 $\text{H}^{\delta 21}$, N9 $\text{H}^{\delta 22}$, A75 H^{β} , T93 $\text{H}^{\gamma 2}$ and T93 H^{β} . With the exception of C6 $\text{H}^{\beta 2}$ and T93 H^{β} , dipolar interactions were observed for all of these protons which could arise also from water 111 besides other water molecules. However, all observed dipolar interactions were of type A/B because the protein environment of water 111 is ‘bristling’ with rapidly exchanging protons in the solution structure of RNase T₁, rendering all possible intermolecular dipolar interactions ambiguous. The $^{13}\text{C}^{\gamma}$ chemical shift of the carboxylate group of D76 does not change much in the pH range of the titration curve (Figure 6). The carboxyl carbons of the other aspartate residues of RNase T₁ appear between 176 and 178 ppm for the protonated state and between 180 and 182 ppm for the deprotonated state. As an example, the titration curve of D49 is shown in Figure 6. (See Pfeiffer et al., 1996 for calibration of the ^{13}C chemical shifts.) The carboxyl carbon of D76 resonates between 178.4 and 178.9 ppm which is halfway between the expected chemical shift values for the protonated and deprotonated state of the carboxyl carbons of aspartate residues in RNase T₁. However, this carboxylate group must be protonated because its environment lacks any positive charge for compensation of a negatively charged (deprotonated) carboxylate group. The increased $^{13}\text{C}^{\gamma}$ chemical shift values therefore suggest that the proton at the carboxylate group is involved in a hydrogen bond, namely with water 111. Regarding the geometry of the crystal structure near D76 (Martinez-Oyanedel et al., 1991) the water molecule 111 might accept a second hydrogen bond, from T93 $\text{O}^{\gamma 1}$ (Figures 7 and 8). In agreement with the NMR data the water protons are too far away from C6 O for hydrogen bonding: the $^1J_{\text{NC}}$ coupling constant of the peptide bond is too small (15.0 ± 0 Hz) for an intermolecular hydrogen bond with a water molecule. The hydroxyl proton of Y11 exhibits a hydrogen bond to the second carboxylate oxygen of D76. This hydrogen bond is supported by the observed downfield shift of the ^1H resonance frequency of this hydroxyl proton compared to a random coil conformation and by the NMR solution structure of RNase T₁. A hydrogen bond between the side-chain amide protons of N9 and D76 O^{δ} was also observed in the solution structure of RNase T₁. This arrangement of the water molecule 111 would be consistent with the NMR data. No resonance distinct from that of water could be identified for the γ -hydroxyl protons of T91 and T93

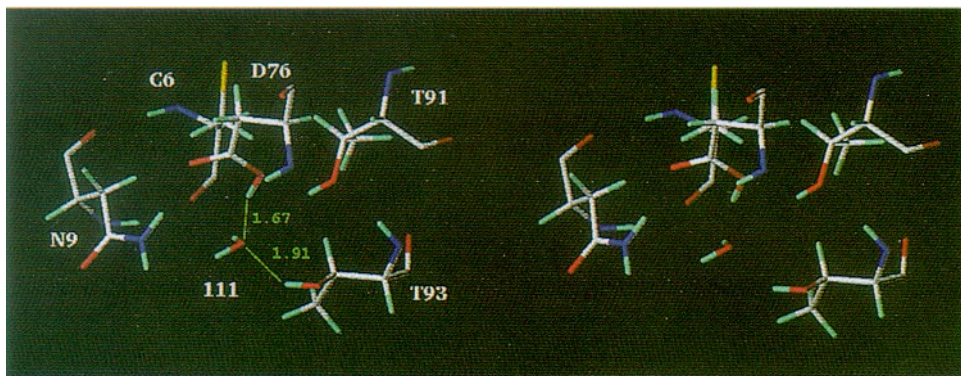


Figure 7. Stereo view of the amino acid residues surrounding the water molecule 111 in the crystal structure of nucleotide-free RNase T₁ (Martinez-Oyanedel et al., 1991). The orientation of the O–H bonds was modelled using the NMR data and a standard energy minimization of SYBYL. The amino acid residues are indicated by the one-letter code and their corresponding sequence position. The length of the two hydrogen bonds involving the water oxygen is given. Sulphur, oxygen, nitrogen and carbon atoms are yellow, red, blue and white, respectively. Protons are coloured cyan.

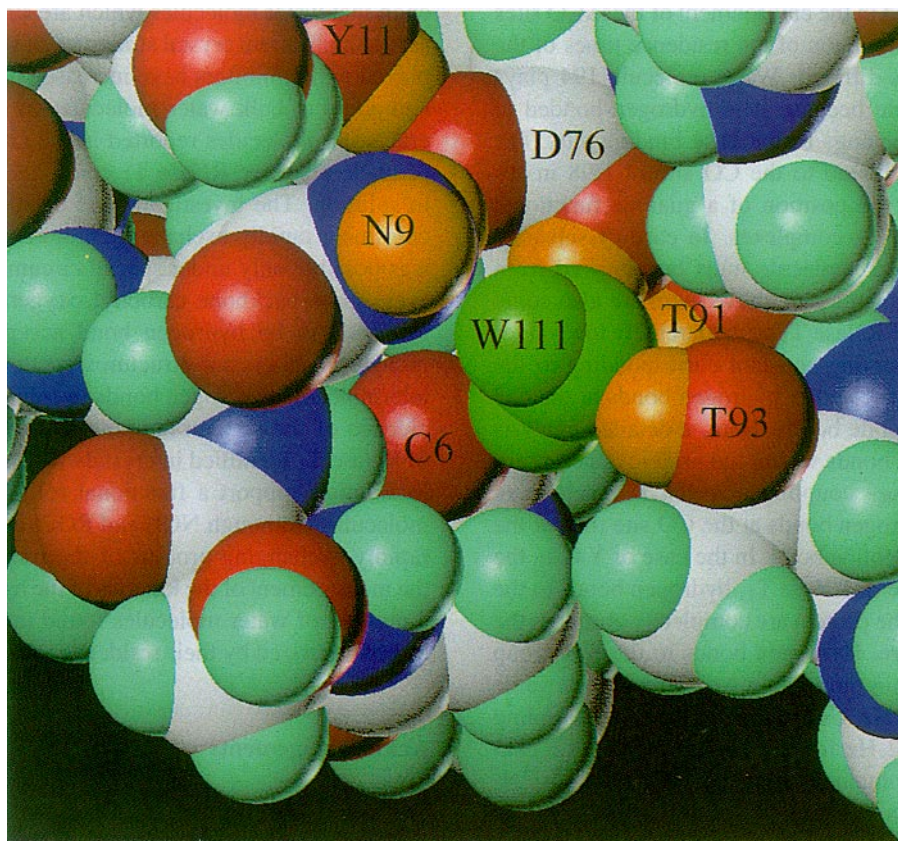


Figure 8. Space-filling representation of the protein surface surrounding the water molecule 111 in the crystal structure of nucleotide-free RNase T₁ (Martinez-Oyanedel et al., 1991). The amino acid residues relevant for hydrogen bonding are indicated by the one-letter code and their corresponding sequence position. Colours of atom types are the same as in Figure 7. In addition, the hydroxyl protons of Y11, T91 and T93 as well as the side-chain amide protons of N9 and the proton at the carboxylate group of D76 are coloured orange. The water molecule 111 is coloured green.

indicating high exchange rates with the solvent ranging between 20 s^{-1} and 103 s^{-1} (Wüthrich, 1986). The hydroxyl group of T91 is located at the bottom of the surface groove 'behind' the water molecule 111 (Figure 8). It is very likely that the water molecule must be removed from the surface-groove to allow for the chemical exchange of T91 H $^{\nu}$. Thus, the experimental data associated with water 111 indicate that it is not as tightly bound to RNase T₁ as suggested from the crystal structures. It should be remembered at this point that we investigated RNase T₁ in solution without calcium ions (Ca²⁺). In the crystal structures of RNase T₁, the calcium ion is co-ordinated at the D15 carboxylate in the neighbourhood of D76. Small changes of the hydration due to the absence of the calcium ion are imaginable.

Some water molecules are hydrogen-bonded to backbone CO (or NH sites) in solution (Table 1). Frequently, no unambiguous NOE or ROE interaction could be detected in the environment of these CO sites rendering the estimation of the residence times of the water molecules difficult. Water molecule 194 plays an important role because it is hydrogen-bonded to N98 O which belongs to the base binding site. The water molecule bound to the CO site of N98 in solution occupies the position of a guanine functional group in RNase T₁ complexes. In case of substrate binding this water molecule must be removed from the protein. As mentioned above there are also some peptide bonds of RNase T₁ with extremely low values of the $^1J_{\text{NC}'}$ coupling constant corresponding to the absence of intermolecular hydrogen bonds at the CO site of these peptide bonds. Here, a detailed analysis of the hydrogen bonds within the protein is necessary because the $^1J_{\text{NC}'}$ coupling constant is much more sensitive to hydrogen bonds at the CO site than at the NH site of the peptide bond. In the case of Y42 in the base binding site of RNase T₁, hydrogen bonds to the CO site within the protein are completely absent in the solution structure. Hydrogen bonds to the NH group exclusively within the protein would result in a value of $^1J_{\text{NC}'} \geq 13.5 \text{ Hz}$. Unfortunately, the $^1J_{\text{NC}'}$ coupling constant of 13.2 Hz for the peptide bond Y42–N43 could only be obtained from the $^{13}\text{C}'$ -coupled ^{15}N -HSQC spectrum because of spectral overlap in the 2D H(CA)CO experiment. A possible negative cross peak due to a ROE interaction between water and the backbone amide proton of N43 is overlaid by the magnetization transfer due to the fast chemical exchange of this amide proton. Despite the observed positive ROE cross peak for N43 H^N in the H₂O-ROE- ^{15}N -HSQC

difference experiment, it seems to be possible that a short-living water molecule forms a hydrogen bond to this amide proton, namely the water molecule 140. The position of water 140 in nucleotide-free RNase T₁ is equivalent to guanine N7 in RNase T₁ complexes. In contrast to the crystal structure of nucleotide-free RNase T₁ no water molecule binds simultaneously to the CO sites of Y42 and N43 in the base binding site in solution. It can be assumed that these missing intermolecular hydrogen bonds for water 129 (bridging Y42 O and N43 O) and 140 (bridging Y43 O and Y43 H^N) might cause increased flexibility of the tripeptide Y42–N43–N44 as described previously for the solution structure of RNase T₁ (Pfeiffer et al., 1997).

Conclusions

In summary, this NMR study supports the phenomenon that water molecules which are structurally conserved in different crystal structures of RNase T₁ complexed with inhibitors have increased residence times compared to bulk water molecules in solution. Several water molecules reported in the crystal structure of nucleotide-free RNase T₁ could also be identified in solution. The investigation of crystal water molecules near rapidly exchanging protons of the enzyme was possible only under special circumstances. However, some backbone carbonyl oxygens which were supposed to be hydrogen bond acceptors of water molecules in crystal structures seem to exhibit no intermolecular hydrogen bonds in solution. The coincidence of the structurally conserved hydration sites of RNase T₁ identified in crystals with those observed in solution support a functional role of these water molecules. Although NOE and ROE interactions with rapidly exchanging protons of the protein may limit the measurement of the kinetics of the hydration water, a number of water molecules found in crystals could be characterized by their residence times in solution.

Acknowledgements

We would like to thank the Deutsche Forschungsgemeinschaft for a grant (Ru 145/8–6, Ru 145/12–2). We also thank Dr Nenad Juranić, Mayo Graduate School Rochester, for helpful discussions.

References

- Abragam, A. (1961) *Principles of Nuclear Magnetism*, Clarendon Press, Oxford.
- Arata, Y., Kimura, S., Matsuo, H. and Narita, K. (1976) *Biochem. Biophys. Res. Commun.*, **73**, 133–140.
- Berger, S. (1978) *Tetrahedron*, 3133–3136.
- Billeter, M. (1995) *Prog. NMR Spectrosc.*, **27**, 635–645.
- Bothner-By, A.A., Stephens, R.L., Lee, J., Warren, C.D. and Jeanloz, R.W. (1985) *J. Am. Chem. Soc.*, **106**, 811–818.
- Brüschweiler, R. and Wright, P.E. (1994) *Chem. Phys. Lett.*, **229**, 75–81.
- Clore, G.M., Bax, A., Wingfield, P.T. and Gronenborn A.M. (1990) *Biochemistry*, **29**, 5671–5676.
- Clore, G.M., Bax, A., Omichinski, J.G. and Gronenborn, A.M. (1994) *Structure*, **2**, 89–94.
- Davis, A.L., Keefer, J., Laue, E.D. and Moskau, D. (1992) *J. Magn. Reson.*, **98**, 207–216.
- Delaglio, F., Torchia, D.A. and Bax, A. (1991) *J. Biomol. NMR*, **1**, 439–446.
- Denisov, V.P. and Halle, B. (1995a) *J. Mol. Biol.*, **245**, 682–697.
- Denisov, V.P. and Halle, B. (1995b) *J. Mol. Biol.*, **245**, 698–709.
- Denisov, V.P., Halle, B., Peters, J. and Hörlein, H.D. (1995) *Biochemistry*, **34**, 9046–9051.
- Eberhardt, E.S. and Rains, R.T. (1994) *J. Am. Chem. Soc.*, **116**, 2149–2152.
- Edsall, J.T. and McKenzie, H.A. (1983) *Adv. Biophys.*, **16**, 53–183.
- Egami, F. (1966) *J. Sci. Indust. Res.*, **25**, 442–449.
- Egami, F. and Nakamura, K. (1969) In *Molecular Biology, Biochemistry and Biophysics* (Eds, Kleinzeller, A., Springer, G.F. and Wittmann, H.G.), Springer-Verlag, Berlin, Vol. 6, pp. 1–87.
- Egami, F., Takahashi, K. and Uchida, T. (1964) In *Progress in Nucleic Acid Research and Molecular Biology* (Eds, Davidson, J.N. and Cohn, W.E.), Academic Press, New York, NY, Vol. 3, pp. 59–101.
- Ernst, R.R., Bodenhausen, G. and Wokaun, A. (1987) *Principles of Nuclear Magnetic Resonance in One and Two Dimensions*, Clarendon Press, Oxford, Vol. 14, pp. 519–527.
- Finney, J.L. (1979) In *The Physics and Chemistry of Water. A Comprehensive Treatise* (Ed., Frank, F.), Plenum Press, New York, NY, Vol. 6, pp. 47–122.
- Finney, J.L., Goodfellow, J.M. and Poole, P.L. (1982) In *Structural molecular biology. Methods and Applications* (Eds, Davis, D.B., Saenger, W. and Danyluk, S.S.), Plenum Press, New York, NY, pp. 387–426.
- Finney, J.L., Goodfellow, J.M., Howell, P.M. and Vovelle, F. (1985) *J. Biomol. Struct. Dyn.*, **3**, 599–622.
- Grzesiek, S. and Bax, A. (1993a) *J. Am. Chem. Soc.*, **115**, 12593–12594.
- Grzesiek, S. and Bax, A. (1993b) *J. Biomol. NMR*, **3**, 627–638.
- Heinemann, U. and Saenger, W. (1982) *Nature*, **299**, 27–31.
- Jeffrey, G.A. and Saenger, W. (1991) *Hydrogen Bonding in Biological Structures*, Springer-Verlag, Berlin, p. 505.
- Juranić, N., Ilich, P.K. and Macura, S. (1995) *J. Am. Chem. Soc.*, **117**, 405–410.
- Juranić, N., Likic, V.A., Prendergast, F.G. and Macura, S. (1996) *J. Am. Chem. Soc.*, **118**, 7859–7860.
- Kay, L.E., Ikura, M., Tschudin, R. and Bax, A. (1990) *J. Magn. Reson.*, **89**, 496–514.
- Klotz, I.M. and Franzen, J.S. (1962) *J. Am. Chem. Soc.*, **84**, 3641–3646.
- Kraulis, P.J. (1991) *J. Appl. Crystallogr.*, **24**, 946–950.
- Kuntz, I.D. and Kauzmann, W. (1974) *Adv. Protein Chem.*, **28**, 239–345.
- Levitt, M.L. and Park, B.H. (1993) *Structure*, **1**, 223–226.
- Liepinsh, E., Otting, G. and Wüthrich, K. (1992) *J. Biomol. NMR*, **2**, 447–465.
- Llinas, M. and Klein, M.P. (1975) *J. Am. Chem. Soc.*, **97**, 4731–4737.
- Malin, R., Zielenkiewicz, P. and Saenger, W. (1991) *J. Biol. Chem.*, **266**, 4848–4852.
- Martinez-Oyanedel, J., Choe, H.-W., Heinemann, U. and Saenger, W. (1991) *J. Mol. Biol.*, **222**, 335–352.
- Nishikawa, S., Morioka, H., Kim, H.J., Fuchimura, K., Tanaka, T., Uesugi, S., Hakoshima, T., Tomita, K., Ohtsuka, E. and Ikehara, M. (1987) *Biochemistry*, **26**, 8620–8624.
- Otting, G. and Wüthrich, K. (1989) *J. Am. Chem. Soc.*, **111**, 1871–1875.
- Otting, G., Liepinsh, E. and Wüthrich, K. (1991) *Science*, **254**, 974–980.
- Otting, G. and Liepinsh, E. (1995) *Acc. Chem. Res.*, **28**, 171–177.
- Pfeiffer, S., Engelke, J. and Rüterjans, H. (1996) *Quart. Magn. Res. Biol. Med.*, **3**, 69–87.
- Pfeiffer, S., Karimi-Nejad, Y. and Rüterjans, H. (1997) *J. Mol. Biol.*, **266**, 400–423.
- Pfeiffer, S. (1997) Ph.D. Thesis, Johann Wolfgang Goethe University, Frankfurt, Germany.
- Piculle, L. and Halle, B. (1986) *J. Chem. Soc. Faraday Trans.*, **182**, 401–414.
- Piotto, M., Saudek, V. and Sklenar, V. (1992) *J. Biomol. NMR*, **2**, 661–665.
- Rupley, J.A., Gratton, E. and Careri, G. (1983) *Trends Biol. Sci.*, **8**, 18–22.
- Solomon, F. (1955) *Phys. Rev.*, **99**, 559–565.
- Sugio, S., Amisaki, T., Ohishi, H. and Tomita, K. (1988) *Biochemistry*, **103**, 354–366.
- Takahashi, K. (1965) *J. Biol. Chem.*, **240**, 4117–4119.
- Takahashi, K., Stein, W.H. and Moore, S. (1967) *J. Biol. Chem.*, **242**, 4682–4690.
- Takahashi, K. (1970) *Biochemistry*, **68**, 659–664.
- Takahashi, K. (1973) *Biochemistry*, **74**, 1279–1282.
- Takahashi, K. (1976) *Biochemistry*, **80**, 1267–1275.
- Thanki, N., Thornton, J.M. and Goodfellow, J.M. (1988) *J. Mol. Biol.*, **202**, 637–657.
- Vuister, G.W. and Bax, A. (1992) *J. Magn. Reson.*, **98**, 428–435.
- Walter, J.A. and Wright, L.C. (1979) *Tetrahedron Lett.*, **41**, 3909–3912.
- Wang, Y.-X., Freedberg, D.J., Grzesiek, S., Torchia, D.A., Wingfield, P.T., Kaufman, J.D., Stahl, S.J., Chang, C.-H. and Hodge, C.N. (1996) *Biochemistry*, **35**, 12694–12704.
- Westhof, E. (1993) *Water and Biological Macromolecules*, Macmillan, London, pp. 63–159.
- Wüthrich, K. (1986) *NMR of Proteins and Nucleic Acids*, John Wiley and Sons Inc., New York, NY, p. 24.